



This is a repository copy of *Assessing uncertainty in housing stock infiltration rates and associated heat loss: English and UK case studies*.

White Rose Research Online URL for this paper:
<http://eprints.whiterose.ac.uk/127462/>

Version: Submitted Version

Article:

Jones, B., Das, P., Chalabi, Z. et al. (6 more authors) (2015) Assessing uncertainty in housing stock infiltration rates and associated heat loss: English and UK case studies. *Building and Environment*, 92. pp. 644-656. ISSN 0360-1323

<https://doi.org/10.1016/j.buildenv.2015.05.033>

Reuse

This article is distributed under the terms of the Creative Commons Attribution-NonCommercial-NoDerivs (CC BY-NC-ND) licence. This licence only allows you to download this work and share it with others as long as you credit the authors, but you can't change the article in any way or use it commercially. More information and the full terms of the licence here: <https://creativecommons.org/licenses/>

Takedown

If you consider content in White Rose Research Online to be in breach of UK law, please notify us by emailing eprints@whiterose.ac.uk including the URL of the record and the reason for the withdrawal request.



eprints@whiterose.ac.uk
<https://eprints.whiterose.ac.uk/>

ASSESSING UNCERTAINTY IN HOUSING STOCK INFILTRATION RATES AND ASSOCIATED HEAT LOSS: ENGLISH AND UK CASE STUDIES

Benjamin Jones^{*1}

Payel Das²

Zaid Chalabi³

Michael Davies⁴

Ian Hamilton⁵

Robert Lowe⁵

Anna Mavrogianni⁴

Darren Robinson¹

Jonathon Taylor⁴

1. Department of Architecture and Built Environment, University of Nottingham, Nottingham, NG7 2RD, United Kingdom
2. Rudolf Peierls Centre for Theoretical Physics, University of Oxford, 1 Keble Road, Oxford, OX1 3NP, United Kingdom
3. London School of Hygiene & Tropical Medicine, 15-17 Tavistock Place, London, WC1H 9SH, United Kingdom
4. UCL Institute for Environmental Design and Engineering, The Bartlett, University College London, Central House, 14 Upper Woburn Place, London, WC1H 0NN, United Kingdom
5. UCL Energy Institute, The Bartlett, University College London, Central House, 14 Upper Woburn Place, London, WC1H 0NN, United Kingdom

*Corresponding author: benjamin.jones@nottingham.ac.uk

ABSTRACT

Strategies to reduce domestic heating loads by minimizing the infiltration of cold air through adventitious openings located in the thermal envelopes of houses are highlighted by the building codes of many countries. Consequent reductions of energy demand and CO₂e emission are often unquantified by empirical evidence. Instead, a mean heating season infiltration rate is commonly inferred from an air leakage rate using a simple ratio scaled to account for the physical and environmental properties of a dwelling. The scaling does not take account of the permeability of party walls in conjoined dwellings and so cannot differentiate between the infiltration of unconditioned ambient air that requires heating, and conditioned air from adjacent dwellings that does not.

A stochastic method is presented that applies a theoretical model of adventitious infiltration to predict distributions of mean infiltration rates and the associated total heat loss in any stock of dwellings during heating hours. The method is applied to the English and UK housing stocks and provides probability distribution functions of stock infiltration rates and total heat loss during the heating season for two extremes of party wall permeability. The distributions predict that up to 79% of the current English stock could require additional purpose-provided ventilation to limit negative health consequences. National models predict that fewer dwellings are under-ventilated. The distributions are also used to predict that infiltration is responsible for 3-5% of total UK energy demand, 11-15% of UK housing stock energy demand, and 10-14% of UK housing stock carbon emissions.

HIGHLIGHTS

- Heating season infiltration and heat loss distributions for English housing stock.
- Up to 79% of English dwellings may be under ventilated.
- Exfiltration estimated to be responsible for 3-5% of total UK energy demand.
- Exfiltration estimated to be responsible for 11-15% UK housing stock energy demand.
- Exfiltration estimated to be responsible for 10-14% UK housing stock CO₂ emissions.

KEYWORDS

Ventilation, Permeability, Leakage, Model, Monte Carlo, DOMVENT

1 INTRODUCTION

Many countries are obligated to reduce their greenhouse gas (GHG) emission rates in order to limit the effects of climate change. The UK is legally required by its Climate Change Act [1] to reduce its 1990 GHG emissions by 80% by 2050. A reduction in the energy demand of the domestic housing stock, which accounts for more than a quarter of UK energy demand and GHG emissions [2], is a primary target for cuts via the Green Deal home improvement scheme [3-4]. One strategy is to reduce domestic heating loads by minimizing the infiltration of cold air and the concurrent exfiltration of conditioned air through adventitious (unintentional) openings located in the thermal envelope. Although logical, this strategy cannot be said to be based on empirical evidence that provides measurements of mean infiltration rates during the heating season and associated heat loss. Instead, measurements of ventilation are presented that combine adventitious and purpose-provided (intentional) ventilation (PPV) [2,5], or are for individual houses [6-7] that are not necessarily representative of the broader housing stock [8]. This is perhaps understandable, because the longitudinal measurement of infiltration is challenging. Therefore, the resistance of the thermal envelope to airflow is assessed by artificially and systematically increasing the difference between the internal and external air pressures ΔP (Pa) and measuring the airflow rate \dot{V} (m³/h) across it. These parameters are conventionally related by a power law

$$\dot{V} = a\{\Delta P\}^b \quad (1)$$

where a ($\text{m}^3/\text{h}/\text{Pa}^b$) and b are a flow coefficient and flow exponent, respectively, determined by regression [9-10]. It is common to report \dot{V} at 50Pa, interpolated from measurements, when it is known as an air leakage rate (ALR), \dot{V}_{50} (m^3/h). In order to compare ALRs measured in different buildings, it is normalized by a common parameter, such as building volume to become an air change rate N_{50} (h^{-1}), or by the thermal envelope area to become an Air Permeability, Q_{50} ($\text{m}^3/\text{h}/\text{m}^2$)¹ [9-11]. Many building codes state limiting values of N_{50} or Q_{50} ; for example, a Q_{50} of $10\text{m}^3/\text{h}/\text{m}^2$ is the maximum permissible for a new UK dwelling [12].

Operational pressure differences are typically an order of magnitude lower than 50Pa at around 4Pa, and here Etheridge [13] argues that an acceptable value of Q_4 is implicit in the acceptable value of Q_{50} because one can be estimated from the other if b is known. The standard procedure used to determine a and b measures \dot{V} at intervals between $10 \leq \Delta P \leq 100\text{Pa}$ [9-10] to limit the effect of noise from naturally occurring wind and buoyancy on the measurement of the air leakage rate. Systematic uncertainty arises from the fact that the shape of the leakage characteristic is not known when $0 < \Delta P < 10\text{Pa}$ and here Equation (1) may not hold [13]. A new measurement procedure may be required that satisfies this knowledge gap [14-15]. Nevertheless, these uncertainties mean that a value of Q_4 , extrapolated from the high pressure measurements, is not used directly to predict an operational infiltration rate. Instead, other empirical relationships are used that relate \dot{V}_{50} to a mean heating season infiltration rate \bar{V}_I (m^3/h), often by a simple ratio known as the *leakage-infiltration ratio*, L [16].

$$(\dot{V}_{50}/\bar{V}_I = Q_{50}/\bar{Q}_I = N_{50}/\bar{N}_I) \approx L. \quad (2)$$

L is frequently taken to be equal to 20 and then scaled; for example, the National Building Code of Finland [17] uses $L=20$ for 3 and 4 storey dwellings and increases L as the number of storeys reduces. Similarly, British Standard 5925 [18] states, without reference, that $N_{50}/20$ is an indicator of the average heating season infiltration rate in UK dwellings, \bar{N}_I . The UK government's method of assessing the energy performance of dwellings is the Standard Assessment Procedure (SAP) and is

¹ We note that this formulation cancels unproblematically to m^3/h , which has a simple and obvious physical interpretation. However, the units of $\text{m}^3/\text{h}/\text{m}^2$ are those most commonly ascribed to air permeability and so are used herein.

based on the Building Research Establishment Domestic Energy Model (BREDEM) domestic energy model [19]. Both SAP and BREDEM apply $L=20$ in the first instance and attribute further infiltration (unmeasured by an air leakage test) to fans, chimneys, and ducts, and scale the total infiltration rate according to the average wind speed and the number of sheltered sides.

The application of a steady-state weather-independent measurement of airflow to predict one that is highly dynamic and weather dependent is obviously problematic and concern about the widespread use of this heuristic has been raised. For example, Jones *et al.* [20] identify great uncertainty in its predictions for conjoined (multi-family) dwellings, and that it cannot be used to differentiate between the infiltration of unconditioned ambient air that requires heating and conditioned air from an adjacent dwelling. This is a phenomenon that has been highlighted by *guarded zone* tests in apartments where the airflow through party wall accounts for 31-58% of the total air leakage rate [21]; see [20] for further examples. Jones *et al.* [20] propose that two extreme assumptions can be made about the permeability of party walls of a dwelling at 50Pa indicated by their relative permeability \tilde{Q} : $A(\tilde{Q} = 1)$ the party walls have the same permeability as the dwelling and so airflow to and from adjacent dwellings does occur; or $A(\tilde{Q} = 0)$ the party walls are impermeable and so airflow to and from adjacent dwellings does not occur. Using a theoretical approach the authors predict for assumption $A(\tilde{Q} = 1)$ that L is significantly higher than that used by building codes whereas for assumption $A(\tilde{Q} = 0)$ L is predicted to be close to that used in practice. The consequences of these findings are two-fold. Firstly, if $A(\tilde{Q} = 1)$ is true, then operational heat losses are less than those predicted by models that apply L , and government-funded schemes that aim to tighten the European housing stock could have longer payback periods than expected. Secondly, if $A(\tilde{Q} = 0)$ is true, the same schemes may be appropriate.

This predicted divergence of outcomes introduces great uncertainty into the effectiveness of any policy that aims to reduce energy demand through fabric tightening and there is a need to determine the distribution of infiltration rates in stocks of houses that have a large number of multi-family dwellings. To do this, an exhaustive field survey is required to give a reliable empirical basis for the prediction of \bar{N}_I or \bar{Q}_I from dwelling characteristics; see Chan *et al.* [22] who analyse the sizeable US air leakage database (of size $n=70,000$). In the short term, a modelling approach, such as that

described by Persily *et al.* [8], provides an easier means of predicting the distribution of infiltration rates in a stock of dwellings using all available data as inputs. The data generated by the model can be used to investigate the likely forms of, and uncertainties in, relationships between N_{50} and \bar{N}_I .

Accordingly, this article uses a stochastic approach to generate distributions of mean infiltration rate during heating hours and total exfiltration heat loss for both extreme party wall permeability assumptions for the English housing stock, although the method can be applied to any stock. The energy demand and carbon emissions for the larger UK housing stock are also estimated. It does this by using an existing model of dwelling infiltration and exfiltration informed by sources of quantitative data. Both the model and its inputs are discussed in Section 2. In Section 3 they are used to generate the distributions, and in Section 4 the predictions are used to investigate the usefulness of L and of other simplified models that apply it. Finally, the sensitivity of the model to its inputs is assessed in Section 5.

2 METHODS

There are no known large-scale measurements or models of heating season infiltration rates in English dwellings and so a modelling approach is proposed. An infiltration model requires three things: a generic model of dwelling infiltration and exfiltration, knowledge of the properties of a large representative sample of a dwelling stock that can be applied to the model, and a suitable statistical approach that enables the stock variability and parametric uncertainty to be captured (measurements of dwelling properties reflect both). The three requirements are discussed using the English housing stock as a case study, although the approach is readily transferable to housing stocks in other countries. Figure 1 shows the proportion of the dwelling types that comprise the English stock. Generally, detached houses do not share walls with adjacent dwellings, semi-detached and end-of-terrace houses share one vertical wall with adjacent dwellings, mid-terrace houses share at least two vertical walls, and apartments share up to five of their horizontal and vertical surfaces. Accordingly, Figure 1 shows that 78% of the English stock shares at least one of their external surfaces with another dwelling and so any difference between predictions for the two permeability assumptions $A(\tilde{Q} = 1)$ and $A(\tilde{Q} = 0)$ is expected to be clearly observed in four of the five dwelling types.

In this section, a model of infiltration and exfiltration heat loss during the heating season is selected, suitable sources of input data are identified, a method of obtaining suitable distributions is established, and existing simplified models of infiltration are defined for comparison. Finally, a methodology is given to test the dependence of the model's outputs on its inputs.

2.1 Modelling infiltration and exfiltration heat loss

For any model there is always a trade-off between model complexity and data on one hand and computational speed on the other. Variations in the predictions of a model are a function of stock variability, parametric uncertainty (uncertainties in the inputs to the model), and structural uncertainty (uncertainty in the model formulation itself). When modelling a stock of dwellings, the sample size is expected to be large and so a computationally fast model is desirable. Furthermore, the variation in geometry types across a stock dictates that the model should also be versatile. A final requirement is that the workings and limitations of the model must be documented and its predictions compared against empirical data or, less desirably, corroborated against the predictions of other models.

This article applies DOMVENT3D, a model of infiltration and exfiltration through any number of façades developed initially by Lowe [23] on the basis of a theoretical formulation by Lyberg [24], and subsequently extended by Jones *et al.* [25]. It assumes two things about those façades: all are uniformly porous; and the pressure distribution over a vertical surface is linear. DOMVENT3D integrates the airflow rate in the vertical plane to predict the total airflow rate through any number of façades [25]. DOMVENT3D makes further assumptions about the dwelling. Following Etheridge [13], it assumes that all rooms are interconnected and internal flow resistances are negligible. Each horizontal and vertical surface of the external envelope requires only a single flow equation linked by a continuity equation, thus reducing computational time. DOMVENT3D's final assumption follows Jones *et al.* [20] who state that adjacent dwellings are assumed to experience identical environmental conditions and thus have the same internal air pressure. Therefore, airflow through permeable party walls and floors does not occur under operational conditions and so is only considered through external surfaces. DOMVENT3D is implemented using bespoke MATLAB code [26] available online [27]. Its assumptions, merits (including advantages over other models of infiltration), limitations, and

the corroboration of its predictions are discussed briefly in Appendix A and in depth elsewhere [20,25].

DOMVENT3D requires inputs that may be unique to a dwelling or are general to a sub-stock of dwellings bounded by a geographic region. Unique inputs comprise the flow exponent, internal air density, the dimensions of all permeable external vertical (façades) and horizontal (ceilings and floors) surfaces, scaled wind speed (by building height and terrain), and façade wind pressure coefficients. General inputs are the altitude, ambient air temperature T_{ext} (°C), regional wind speed, and wind orientation. Where appropriate, airflow constants are calculated using ASHRAE Standard Atmospheric Conditions [28]. Other sources of data are discussed in Section 2.2.

The exfiltration heat loss $H(t)$ (W) at an instant in time t is estimated by

$$H(t) = \dot{V}_I(t)\bar{\rho}(t)c\Delta T(t)\Big|_{\{T_{int}(t)-T_{ext}(t)\}\geq 3} \quad (3)$$

where \dot{V}_I (m^3/s) is the infiltration rate, $\bar{\rho}$ (kg/m^3) is the mean of the internal and external air densities, c is the specific heat capacity of air ($\text{Jkg}^{-1}\text{K}^{-1}$), and ΔT (K) is the difference between the internal and ambient air temperatures. The internal air temperature, T_{int} (°C), of a typical unheated English house is, on average, approximately 3°C higher than T_{ext} ; the difference is attributable to solar and casual heat gains and fabric properties that affect heat transfer and thermal inertia. Therefore, the heating system is assumed to function only when T_{ext} is at least 3°C below T_{int} [29-31]. Equation (3) is integrated over the entire heating season to estimate the total heat loss, H_I (kWh) via exfiltration.

2.2 Model inputs

The English housing stock comprises 22.3 million dwellings, of which a statistically representative sample of 16,150 dwellings is documented by the 2009 English Housing Survey (EHS) [32]. Geometric, physical, and environmental information is given for each sample. Although the EHS is data rich, DOMVENT3D's inputs are not always explicitly available and so metadata must be derived from the EHS and other sources, or assumed. Inputs to DOMVENT3D may be divided into three distinct types and are tabulated in Appendix B: geometric (dwelling dimensions, dimensions of blocks of dwellings, and orientation), physical (Q_{50} , b , and façade pressure coefficients), and environmental

(location, local wind speed and direction, internal and ambient temperatures, terrain type, and local shielding) parameters. Correlations between the input parameters are considered in Section 2.5. Each metadata type is discussed in turn, beginning with geometric data.

2.2.1 Geometric metadata

The EHS assumes that two connecting cuboids can reasonably represent the geometry of ~98% of English dwellings [33]. The proportion of each surface shared with another dwelling is given and is not always 100%; for example, a terraced house might be staggered in the horizontal plane. The cuboid model is constructed following the Cambridge Housing Model (CHM) [34] used to estimate the energy demand and equivalent carbon dioxide (CO₂e) emissions of the UK housing stock [2]. While the EHS gives significant information about each of the sampled dwellings, it is not always desirable to apply it directly. For example, although the EHS gives the number of storeys in an apartment block and the vertical location of the apartment within the block, there is no evidence that this vertical location is important. Accordingly, the vertical location of the apartment is a random variable uniformly sampled between the boundaries of the block dimensions and commensurate with the number of apartment floors (some have several floors). Dwelling orientation is not given by the EHS and so it is assumed to be a uniformly distributed random variable between $0 \leq \alpha < 360$ degrees (°). Other geometric parameters must also be assumed; for example, the number of dwellings in a block of apartments informs the calculation of physical parameters, such as wind pressure coefficients (see Section 2.2.3), but is not always given by the EHS. In the absence of any direct measurement of the aspect ratio (*AR*) of a block of terraced houses or apartments (a ratio of block width to depth), the number of dwellings in a block is arbitrarily assumed to be a uniformly distributed random variable between 3 and 20. The minimum is chosen because it is the smallest number of houses that can comprise a terrace, and in the absence of evidence, the maximum is an arbitrary large integer. Variable inputs introduce a distribution of outputs that enables a sensitivity analysis to be undertaken in Section 5 to evaluate their impact on the predictions of DOMVENT3D. All geometric inputs are given in Table B1.

2.2.2 Physical metadata

To the best of the authors' knowledge, there are no large-scale measurements of operational infiltration rates in the English housing stock. However, there are a limited number of databases of Q_{50} values for UK dwellings and the biggest two are applied here. Pan [35] gives a histogram of Q_{50} values for 287 new English houses constructed after 2006, and Stephen [36] gives a histogram of Q_{50} values for 384 UK dwellings (also reported in [37]) constructed before 2000. Although there is a requirement to record Q_{50} in a proportion of all dwellings constructed after 2006 [38] they represent a small percentage of the total stock, ~4% [32], and so there is no direct knowledge of Q_{50} for the majority of English dwellings. The existing data [36] shows there is little variation across age bands for houses built before 2000 and so inverse cumulative distribution functions are formed from the published histograms (for all dwelling types together) of Pan and Stephen using Piecewise Cubic Hermite Interpolating Polynomials and are applied if a dwelling is constructed pre-2000 and post-2000, respectively. It is acknowledged that Pan's data is for dwellings constructed post-2006, but its application to post-2000 dwellings is the best compromise that the EHS dwelling age groupings allow. The flow exponent, b , characterises the airflow regime through an air leakage path (ALP) and is a function of its geometry and surface roughness. Its value affects both the pressure difference across an ALP and the airflow rate through it. Most infiltration models assume a constant value of $b = 0.66$ [37], but Sherman [16] shows that a Gaussian distribution with a mean of $\mu=0.65$ and a standard deviation of $\sigma=0.08$ best represents more than 1900 measurements made in U.S. dwellings. Sherman's distribution [16] is very similar to the smaller international AIVC data set [37] and so b is assumed to be a normally-distributed random variable with those parameters safeguarded against negative values. Wind pressure coefficients are defined for the horizontal and vertical surfaces. For the latter, the algorithm of Swami and Chandra [39] gives a normalized average wind pressure coefficient for long-walled low-rise dwellings that is a function of the angle of incidence of the wind (for wind direction see Section 2.2.1), local sheltering (Section 2.2.3), and the block aspect ratio (Section 2.2.1). The coefficient is then scaled to account for local shielding (Section 2.2.3). Horizontal surfaces are assumed to be completely shielded from the effects of the wind following Sherman and Grimsrud [40]. All physical inputs are given in Table B2.

2.2.3 Environmental metadata

The EHS indicates the region in which each sample is located and allows suitable weather data to be chosen. The CIBSE Test Reference Year (TRY) weather data set [41] provides synthesised typical weather years for 10 English regions and is suitable for analysing the environmental performance of buildings. Each EHS region is mapped to an appropriate CIBSE TRY region and where more than one CIBSE region is located in an EHS region it is chosen randomly (with equal probability) from all possible regions. Local altitude, wind speed, wind direction, and ambient air temperature are taken from a CIBSE TRY file (see Section 2.2.2) but the wind speed must be scaled according to the terrain and dwelling height using a standard power law formula (see BSI [18]). Dwelling height is obtained from the cuboid model and the terrain is indicated by the EHS. The four BSI terrain types [18] and the local wind pressure shielding coefficients of Deru and Burns [42] are mapped to the six EHS terrain types; see Table B3.

DOMVENT3D is not a thermal model and treats the internal air temperature as an exogenous variable. Here, a normal distribution of thermostat temperatures (T_{int}) is chosen with $\mu=21.1^{\circ}\text{C}$ and $\sigma=2.5^{\circ}\text{C}$ following Shipworth *et al.* [43] who calculate these values from measurements made in a representative sample of 196 English dwellings. It is acknowledged that, in practice, a heating system may not function all day nor provide a constant air temperature throughout a dwelling. Neither the chosen model nor the available data allows these factors to be accounted for, and so the application of this distribution may overestimate the internal air temperature in English dwellings. Therefore, the sensitivity of DOMVENT3D to this input is investigated in Section 5. All environmental inputs are given in Table B3.

2.3 Stochastic methods

A Monte Carlo approach is used to predict distributions of heating season infiltration and heat loss in English apartments and their sensitivity to model inputs, following the method of Das *et al.* [44]. There are five main stochastic inputs to DOMVENT3D: the EHS variant (using dwelling weight), α , Q_{50} , b , and T_{int} . 100 sets of the five inputs are chosen at a time using a Latin Hypercube [44]. Each set is applied to DOMVENT3D to predict the mean heating season infiltration rate \bar{N}_I (h^{-1}) and the

total heating season heat loss H_I (MWh). The total sample size increases incrementally according to the number of sets, which is chosen to minimize calculation time. After each set of predictions are made, the mean (μ) and standard deviation (σ) of \bar{N}_I for each dwelling type and the whole sample are calculated and used to decide if a stopping criterion has been met. The total number of samples is deemed adequate if the change in μ and σ from one set of 100 samples to the next is less than 0.2% for each dwelling type and for the whole stock. The sample size is chosen to ensure that all dwelling types are considered in each set (a 5-fold increase on that used by Das *et al.* for a single dwelling type), and the stopping criterion is chosen to reflect the lower limit of accuracy of typical ventilation and Indoor Air Quality (IAQ) sensors. The model is run twice because an independent distribution is required for each of the two permeability assumptions, $A(\tilde{Q} = 1)$ and $A(\tilde{Q} = 0)$.

2.4 The BREDEM and SAP models of infiltration

In Section 4 the predictions of DOMVENT3D are compared against those of two national models that apply L ; see Equation (2). BREDEM calculates the energy demand and fuel requirements of dwellings based on its characteristics [19], in accordance with ISO13790 [45]. It is the foundation of models of energy demand given in the literature, such as the Domestic Energy Carbon Model (DECM) [46], the Community Domestic Energy Model (CDEM) [47], and the CHM. SAP is the UK Government's standard approach to the calculation of the energy performance of dwellings [12,48] and is a derivative of BREDEM.

Equations (4) and (5) respectively show how BREDEM and SAP calculate the mean infiltration rate \bar{N}_I (h^{-1}) over a period of time.

$$\bar{N}_{I,BREDEM} = \left(\frac{Q_{50}}{L} + N_{other} \right) \left(\frac{u}{4} \right) C_s C_d \quad (4)$$

$$\bar{N}_{I,SAP} = \left(\frac{Q_{50}}{L} + N_{other} \right) \left(\frac{u}{4} \right) (1 - 0.075 C_e) \quad (5)$$

Both BREDEM and SAP make an initial estimate of infiltration from Q_{50} where $L = 20$, and then add infiltration from other sources, N_{other} (h^{-1}), such as vents and stacks. The direct conversion of Q_{50} ($\text{m}^3/\text{h}/\text{m}^2$) to an air change rate (h^{-1}) either assumes that L has units (m) or, more likely, that the ratio of

dwelling surface area to volume is assumed to be unity. Neither equation accounts for party wall permeability, but their use of $L = 20$ indicates that they implicitly assume party walls to be impermeable [20]. \bar{N}_I is also a function of the mean regional wind speed, u (m/s) (assumed here to be for the period between 1st October and April 30th and taken from tables in [19]) divided by 4m/s. Equation (4) applies two non-dimensional exposure factors (given by tables in [19]) for the site C_s , and the dwelling C_d , whereas Equation (5) reduces the infiltration rate according to the number of exposed sides C_e , and is taken from the EHS, see Section 2.2.2. The mapping of weather regions and sheltering from the EHS to the BREDEM and SAP models is described by tables B1–B3.

2.5 Sensitivity analysis

A sensitivity analysis is required to test the dependence of \bar{N}_I and H_I on DOMVENT3D's inputs. Here, we follow the methodology of Das *et al.* [44] that tests for linear, monotonic, and non-monotonic relationships between inputs and outputs. Associated p values are used to assess whether an input variable is important at a 5% level of significance and three methods are used: correlation, regression, and sample comparison. Relevant outputs and ranking metrics are given in Table 1 of Das *et al.* [44]. For a general overview of the statistics see [49], and for a full and thorough discussion of the statistical tests applied here, see [44].

Three correlation coefficients are employed. Spearman's ranks correlation coefficient (S_{Spear}) measures the strength of the linear correlation between each associated pair of inputs and outputs by calculating how much the variance of each variable can be explained by a monotonic function of the other. Similarly, Kendall's tau (also a rank correlation coefficient, S_{Kend}) measures the strength of the linear correlation between each associated pair of inputs and outputs by calculating the difference between the number of concordant and discordant pairs. We note that this statistic is not used by Das *et al.* but is often found to be less sensitive to outliers than S_{Spear} and so is a useful addition. Pearson's product moment correlation coefficient (S_{Pear}) measures the strength of the monotonic correlation between each related pair of pre-ranked inputs and outputs. All inputs are then ranked according to the magnitude of the correlation coefficient to indicate the level of their importance.

Two regression coefficients are used, and the inputs and outputs are standardized so that they have $\mu = 0$ and $\sigma = 1$. Linear regression ($S_{regress}$) is used to determine the contribution of each input to its related output. This regression is repeated using rank-transformed standardized variables ($S_{rankreg}$). All inputs are ranked according to the magnitude of the regression coefficient.

Two sample-comparison methods are used where the greatest differences between the inputs and outputs indicate relative importance. A two-sample Kolmogorov-Smirnov (KS) test (S_{Kolm}) sorts the outputs by the ascending order of their corresponding inputs and then calculates the maximum vertical distance between the cumulative distribution functions (CDF) of two equal subsamples of the output. The Kruskal-Wallis test ($S_{Krusk\#}$ where # denotes the number of subsamples) divides the inputs into subsamples according to quantiles in the distribution of the outputs and compares the variance within and between each subsample.

A fundamental assumption is that all inputs (see Table 4) are independent of each other, and so any that are themselves correlated are combined. Furthermore, all inputs are ordinal and continuous variables chosen to represent implicitly geometric ($A_I: A_{50}$, $A:V$, AR , α), physical (Q_{50} , b), and environmental (u , ΔT) parameters discussed in Section 2.2. Low correlation between them is confirmed using Kendall's tau.

3 RESULTS

Figures 2 and 3 respectively show the CDFs and probability density functions (PDF) of the mean infiltration rate \bar{N}_I (h^{-1}), and the total exfiltration heat loss H_I (MWh), in English dwellings during the heating season for both permeability assumptions. Here, permeability assumption $A(\tilde{Q} = 1)$ is indicated by the continuous line and $A(\tilde{Q} = 0)$ by the dotted line. Tables 1 and 2 give descriptive statistics for each sample and permeability assumption by dwelling type and for the whole stock. They are also shown in Figure 4 where the lower and upper bars are the 2nd and 98th centiles, the central box bounds the inter-quartile range, the central bar is the median, and the cross is the sample mean. The number of samples required for convergence were 9000 and 10200 for $A(\tilde{Q} = 1)$ and $A(\tilde{Q} = 0)$, respectively. Tables 1 and 2, and Figures 2 and 3 show that all distributions are positively skewed and so the sample medians are used hereon; see Table 3.

Figures 2 and 3 show that the permeability assumptions effect the predicted distributions of \bar{N}_I and H_I for the English housing stock and are predicted to be lower for permeability assumption $A(\tilde{Q} = 1)$ than for $A(\tilde{Q} = 0)$. Assumption $A(\tilde{Q} = 0)$ increases the variance of the sample, indicated by σ . A two-sample KS test is used to test the null hypothesis that the $A(\tilde{Q} = 1)$ and $A(\tilde{Q} = 0)$ samples are from the same continuous distribution against the alternative that they are not. The null hypothesis is rejected at 5% significance for \bar{N}_I ($p < 10^{-6}$) and H_I ($p < 10^{-6}$) indicating that the two \bar{N}_I distributions and two H_I distributions are different. Identical tests for each subsample (by dwelling type) are also rejected, except for the detached dwelling CDFs where the KS test shows that the two \bar{N}_I ($p = 0.021$) and two H_I ($p = 0.076$) distributions are related at 2% and 5% significance, respectively.

3.1 Infiltration

Table 1 shows that the infiltration rate in an English dwelling is predicted to be $0.02 \leq \bar{N}_I \leq 1.24\text{h}^{-1}$ with 96% certainty, whatever the permeability assumption. The differences in predicted \bar{N}_I for assumptions $A(\tilde{Q} = 1)$ and $A(\tilde{Q} = 0)$ in conjoined dwellings can be explained by considering the dwelling surface area that allows airflow at 50Pa, A_{50} (m^2), and under operational conditions, A_I (m^2), for each permeability assumption. The sum of the cross sectional areas of all ALPs is constant, whatever the permeability assumption, if the dwelling permeability is also constant. For assumption $A(\tilde{Q} = 1)$ the party walls are permeable and so ALPs are uniformly located in all surfaces. However, under operational conditions airflow is only assumed to occur through external surfaces (see Section 2.1), and so some ALPs that allow airflow at 50Pa will not allow it under operational conditions ($A_{50} > A_I$). For assumption $A(\tilde{Q} = 0)$ the party walls are impermeable and so all ALPs are located in external surfaces where they allow airflow at 50Pa and under operational conditions ($A_{50} = A_I$). The infiltration rate for $A(\tilde{Q} = 0)$ is expected to be greater than $A(\tilde{Q} = 1)$ because more ALPs are located in external surfaces. Jones *et al.* [20] show the ratio of the predicted infiltration rates for the two permeability assumptions is equal to a ratio of permeable envelope area at a pressure differential of 50Pa A_{50} (m^2), where

$$A_{50,A(\tilde{Q}=0)}/A_{50,A(\tilde{Q}=1)} = \bar{N}_{I,A(\tilde{Q}=1)}/\bar{N}_{I,A(\tilde{Q}=0)} \quad (6)$$

Here, the subscripts indicate the pressure differential and the permeability assumption. Equation (6) shows that apartments are likely to have a ratio $\ll 1$ because they have at least one party wall and so $A_{50,A(\tilde{Q}=1)} \gg A_{50,A(\tilde{Q}=0)}$. For detached houses, the ratio approaches unity because they have no party walls and so $A_{50,A(\tilde{Q}=1)} \approx A_{50,A(\tilde{Q}=0)}$. Note that Equation (6) is valid for a single dwelling and not for an entire distribution. Therefore it is reassuring that Table 3 (last two rows) shows that Equation (6) is approximately true for the $A(\tilde{Q} = 1)$ and $A(\tilde{Q} = 0)$ sample medians for all dwelling types.

The difference in variance between the samples (indicated by σ) is attributable to the variation of A_{50} governed by the permeability assumptions. For the $A(\tilde{Q} = 1)$ sample, $A_{50} = A$ for the vast majority of cases (dwellings with impermeable solid floors are an exception), whereas for the $A(\tilde{Q} = 0)$ sample, $A_{50} \neq A$ for the majority of apartment, terraced, and semi-detached cases (when at least one party wall is assumed) and the variation is bound by $0 \ll A_{50} \ll A$.

It is currently impossible to state with any certainty the most likely permeability assumption applicable to the English or UK stocks. Nevertheless, a limited number of guarded zone tests ($n = 17$) in UK dwellings [36] that isolate the fraction of total air leakage attributable to party walls may provide an indication. In end-terraced dwellings ($n = 2$) party walls account for 2–18% of total air leakage, 0–19% ($n = 4$) in semi-detached dwellings, 4–27% ($n = 2$) in mid-terraced dwellings, and 0–34% ($n = 9$) in apartments. This suggests that the permeability assumption is closer to $A(\tilde{Q} = 0)$ than $A(\tilde{Q} = 1)$ in apartments but the measurements span the range of $A(\tilde{Q} = 1)$ to $A(\tilde{Q} = 0)$ in the other dwelling types. This emphasises the need for a field survey in the UK following existing methods [50]. Figure 2 suggests that 79% and 63% of dwellings have $\bar{N}_I < 0.5\text{ac/h}$ for $A(\tilde{Q} = 1)$ and $A(\tilde{Q} = 0)$, respectively. This is significant because 0.5ac/h is a threshold ventilation rate (albeit with great uncertainty), recommended by many European countries, below which some negative air-quality related health effects increase [20]. This suggests that effective PPV strategies, such as those described in the UK Government's Approved Document F [51], are required in the majority of English dwellings to minimize health risks to occupants and is an important consideration for policy makers. Figure 5 shows that the LIR, SAP, and BREDEM infiltration models estimate that 51%, 62%, and

72% of dwellings have $\bar{N}_I < 0.5\text{ac/h}$, respectively, highlighting the likelihood of under-ventilation from infiltration alone.

The predictions of \bar{N}_I given in Table 1 have consequences for those who model ventilation and pollutant transport in buildings; see [44,52,53]. These studies implicitly applied permeability assumption $A(\tilde{Q} = 1)$ to their models of ventilation and this has two key consequences. Firstly, Figure 2 shows that their predicted infiltration rates will be lower than those predicted using assumption $A(\tilde{Q} = 0)$. Secondly, this could lead to higher predicted concentrations of pollutants from internal sources and lower concentrations of pollutants from external sources, particularly when there is no PPV. This highlights that knowledge of party wall permeability is both relevant and important. It raises an issue with the current building physics modelling methodology that cannot define ALPs using a single value of Q_{50} or its equivalents.

3.2 Energy and Carbon Emissions

Table 2 shows that heating season infiltration heating demand in an English dwelling is predicted to be $0.08 \leq H_I \leq 9.46\text{MWh}$ with 96% certainty, regardless of the permeability assumption. Table 2 shows that the median total heat losses are 1.33MWh and 1.95MWh for $A(\tilde{Q} = 1)$ and $A(\tilde{Q} = 0)$, respectively, which is equivalent to running approximately eight and eleven 20W light bulbs non-stop for a year, respectively.

It is now possible to use the CDFs given in Figure 3 to estimate the total H_I for the entire English housing stock of 22.3m dwellings. This is done by repeatedly sampling from them using sets of uniform random variables, of a size equal to the number of English dwellings, until the change in μ and σ of the total H_I differs by $<0.01\%$. The total H_I for the entire English housing stock is estimated to be 45.78TWh ($\sigma=0.0098\text{TWh}$) and 60.12TWh ($\sigma=0.0122\text{TWh}$) for $A(\tilde{Q} = 1)$ and $A(\tilde{Q} = 0)$, respectively. Corresponding CO₂e emissions are estimated² to be 11.43MtCO₂e and 15.01MtCO₂e for $A(\tilde{Q} = 1)$ and $A(\tilde{Q} = 0)$, respectively. The UK stock comprises 27.42m dwellings. If the English stock is assumed to be a statistically random subsample of the UK (England, Scotland, Wales, and

² The EHS [32] estimates that 90% of UK dwellings have an efficient gas fired central heating system with an average efficiency of 82.5% [2] while the remaining 10% are assumed to have electric heaters. We use an emissions factor for natural gas of 0.184kgCO₂e/kWh and 0.49kgCO₂e/kWh for *consumed* electricity that includes grid losses [54].

Northern Ireland) stock the same approach predicts that the total H_I for the UK housing stock is 56.2TWh ($\sigma=0.0115$ TWh) and 73.81TWh ($\sigma=0.0151$ TWh) for $A(\tilde{Q} = 1)$ and $A(\tilde{Q} = 0)$, respectively. These predictions can be compared to UK government figures for the total UK energy demand in 2012 [2], where they represent 3.4% and 4.5% of the total UK energy demand (1635TWh for all sectors) or 11.2% and 14.7% of the total energy demand of all UK houses (502TWh). Corresponding CO₂e emissions are estimated to be 14.04MtCO₂e and 18.43MtCO₂e for $A(\tilde{Q} = 1)$ and $A(\tilde{Q} = 0)$, respectively, or 10.2% and 13.5% of the 137MtCO₂e estimated [2] for the whole UK stock.

Official UK Government statistics [2] describing dwelling heat loss are predicted using CHM and SAP and reported using a mean thermal conductance \bar{H}' (W/K), where the \bar{H}' for an average dwelling is 290.4W/K. The contribution of all heating season ventilation (purpose-provided and adventitious) for an average dwelling is estimated to be 73W/K or 25% of dwelling \bar{H}' . We predict that the \bar{H}' attributable to infiltration is 28.3W/K and 37.2W/K for $A(\tilde{Q} = 1)$ and $A(\tilde{Q} = 0)$, respectively. These are 39% and 51% of the ventilation \bar{H}' or 10% and 13% of the dwelling \bar{H}' .

In addition to the infiltration described by Equation (5), SAP accounts for PPV through elements such as fans and windows. This paper does not investigate PPV. However, it is acknowledged that PPV could affect adventitious airflow rates, although any changes are likely to be insignificant in comparison to the PPV airflow rates. The national statistics [2] rely on SAP's implementation of Equation (2) and so the differences between the predictions of SAP and DOMVENT3D are investigated in Section 4. Nevertheless, It is reassuring that the predictions made here appear plausible in the context of the national energy statistics [2].

This analysis of H_I suggests that exfiltration heat loss accounts up to 15% of all dwelling energy demand. The vertical walls of an average UK house are predicted to account for 33% of its heating demand [2] and so infiltration energy demand is comparatively small. The remediation of leaky houses requires skilled labour, is invasive and expensive, and can have unpredictable outcomes. Nevertheless, a pragmatic approach may be to address air tightness when retrofitting other energy efficiency measures, such as insulation (floors, ceilings, and walls) or double glazing. Here, it is important to insure that sufficient PPV is provided to mitigate avoidable negative impacts on indoor air quality and

occupant health [52,53]. This approach may limit potential reductions in H_I and CO_{2e} and so savings would have to be found elsewhere, even in other sectors. Finally, we note that there are no existing measurements or predictions of heating season energy demand attributable to infiltration and exfiltration and so validating field work is required to corroborate these assertions; see Section 4.

4 ASSESSING SIMPLIFIED MODELS

The predictions of DOMVENT3D are now compared against the BREDEM and SAP simplified models given in Equation (2) and Section 2.4. Firstly, Equation (2) is evaluated by the linear regression of \bar{N}_I and N_{50} to estimate L , and key performance statistics are calculated: the Coefficient of Determination (R^2), Root Mean Squared Error (RMSE), and Maximum Absolute Error (MAE). Values of L are given in Table 6 by permeability assumption and dwelling type, along with the performance statistics. Initially these statistics show for assumption $A(\tilde{Q} = 1)$ that there is considerable variability in L between dwelling types, but for assumption $A(\tilde{Q} = 0)$ they show that $L \approx 20$ for all dwelling types. However, the values of R^2 suggest that Equation (2) is a poor model of the relationship between \bar{N}_I and N_{50} for each dwelling type and for the whole stock. Furthermore, the RMSEs and MAEs are large for all dwelling types and for the whole stock when compared to their mean and median statistics (see Table 1); for example Table 6 shows that the smallest RMSE is 3.48h^{-1} for end-terrace dwellings for assumption $A(\tilde{Q} = 1)$, which is 74% greater than the sample mean. An analysis by intervals of dwelling façade height, z_s (m), shows that L decreases with z_s —three intervals of z_s investigated where $z_s \leq 4.8\text{m}$, $4.8 < z_s < 6\text{m}$, and $z_s \geq 6\text{m}$ for all dwellings and each dwelling type by permeability assumption giving 36 subgroups—in 35 of 36 subgroup, but the values of R^2 indicate that the relationships are generally weak ($R^2 < 0.7$ in 33 of 36 subgroups). Further analysis to create subgroups parsed by terrain and shielding types gives no improvement in the performance statistics. When considering the $A(\tilde{Q} = 1)$ and $A(\tilde{Q} = 0)$ samples together, hereon known as the *combined* sample, 93% of the dwellings are located in an urban environment and 77% have heavy shielding (see Table B3), and so it is likely that other parameters are responsible for the variation of \bar{N}_I . A distribution of \bar{N}_I , predicted using Equation (2) and the combined sample, is given in Figure 5

and is purely a function of dwelling geometry and the applied distributions of Q_{50} [35,36]. It predicts that ~50% of dwellings have $\bar{N}_I < 0.5\text{h}^{-1}$.

Next, the inputs of the combined sample are applied to the BREDEM and SAP models (see Section 2.4) and in Table 1 and Figure 5 their distributions of predicted \bar{N}_I are compared against those of the $A(\tilde{Q} = 1)$ and $A(\tilde{Q} = 0)$ distributions. Figure 5 and Equations (4)–(5) show that the exposure and shielding factors (see Section 2.4) reduce the predicted \bar{N}_I when compared to the $L = 20$ distribution, and those constants applied to the BREDEM model have the greatest effect. Both distributions are right skewed and have less variance than the $A(\tilde{Q} = 1)$ and $A(\tilde{Q} = 0)$ samples. The models cannot account for geometric or physical parameters such as party wall permeability; for example, Figure 5 shows that the BREDEM and SAP distributions cross both the $A(\tilde{Q} = 1)$ and $A(\tilde{Q} = 0)$ distributions. Critically, neither the BREDEM nor the SAP distribution is exclusively bounded by the $A(\tilde{Q} = 1)$ and $A(\tilde{Q} = 0)$ distributions. This suggests that the exposure and shielding factors discussed in Section 2.4 are either incorrect or are not exclusively responsible for the variation of \bar{N}_I . Other influential parameters are explored in Section 5.

Of course, this analysis assumes that the DOMVENT3D model makes more accurate predictions than Equation (2), BREDEM, and SAP, which may not be true. Nevertheless, if BREDEM or SAP based models (such as [34,47,48]) are used by those advocating or making policy to estimate the potential national benefits of reducing infiltration heating demand, they will predict a more significant impact than the DOMVENT model.

An alternative model of the relationship between \bar{N}_I and N_{50} may be required using empirical or theoretically generated data. In the long term, an exhaustive field survey is required to give a reliable empirical basis for the prediction of \bar{N}_I from dwelling characteristics following the analysis of Chan *et al.* [22]. In the short term, further work could apply meta-modelling techniques to develop a quick and simple model of the relationship between N_{50} and \bar{N}_I and H_I , which use the predictions given here as training and validation data. This will be the subject of a future paper.

5 SENSITIVITY ANALYSIS

It could be argued that the salient assertions made in Sections 3 and 4 are dependent upon the assumptions made in Section 2. Accordingly, the sensitivity analysis described in Section 2.5 is used to determine the relative importance of inputs to DOMVENT3D.

All of the inputs are perturbed simultaneously by the Latin Hypercube sampling method (see Section 2.3) and so any interactions between them (including those that are synergistic) are accounted for [55]. The relationship between each input and the two outputs are first explored using the scatter plots given in Figure 6 for the combined data set. These show approximate linear relationships (with scatter) between Q_{50} , b , and both outputs. The relationship between $A_I: A_{50}$ and both outputs may be linear, tri-modal, or parabolic. The relationships between u and ΔT and both outputs look parabolic. The relationship between $A:V$ and \bar{N}_I looks either bi-modal or parabolic, whereas $A:V$ looks exponentially related to H_I . Finally, the relationships between AR and both \bar{N}_I and H_I could be exponential, whereas the relationships between α and both outputs looks random. From Figure 5 one can conclude that the relationships between the inputs and outputs are varied and largely non-linear, justifying a broad sensitivity analysis.

The test statistics for the combined data are given in Table 4 for \bar{N}_I and in Table 5 for H_I . They show that Q_{50} and b are ranked highest by all tests for both outputs and that they are approximately linearly related. This shows that the accuracy of these predictions could be improved with more robust distributions of Q_{50} by dwelling age and type; current limitations are discussed in Section 2.2.3. This also shows why b should be recorded when Q_{50} is measured *in-situ*.

Elsewhere, the inputs are consistently ranked by all tests for both \bar{N}_I and H_I , although each output is dependent on different inputs; for example, $A:V$ is more important for predicting H_I than \bar{N}_I . The consistency in the ranks is corroborated by p values that are $\ll 0.05$ for the derived correlation coefficients (S_{Kend} , S_{Pear} , S_{Spear} , S_{Kolm} , and $S_{Krusk\#}$) given in Tables 4 and 5, except for ΔT for S_{Kend} and S_{Spear} where $p > 0.08$. This indicates that the outputs are dependent on all of the inputs to some degree and so meta-modelling techniques should consider all inputs in the first instance.

Nevertheless, it is reassuring that the model is less dependent on AR than many of the other parameters given the arbitrary limits imposed on it in Section 2.2.1.

It is interesting to note that the ranking coefficients for S_{Spear} and $S_{rankreg}$, and S_{Pear} and $S_{regress}$ are equal for all inputs and both outputs. This is because the correlation coefficients used to rank both S_{Spear} and S_{Pear} are, in this case, identical to the regression coefficients used to rank $S_{rankreg}$ and $S_{regress}$.

The non-parametric S_{Kolm} and $S_{Krusk\#}$ tests are used to detect any non-monotonic relationship, but Tables 4 and 5 show that these may not be stronger than the others because the inputs are not ranked in a radically different way.

This analysis shows that there are many parameters that influence the prediction of both \bar{N}_I and H_I and it highlights the limitations of simplified models used to predict \bar{N}_I , such as those given by Equations (2), (4), and (5).

6 CONCLUSIONS

This paper presents a stochastic method for predicting distributions of mean infiltration rates and the associated total heat loss in any stock of dwellings during heating hours. The method is applied to the English and UK housing stocks, which have a significant proportion of multi-family dwellings that share at least one of their external surfaces with another, based on two extreme assumptions of party wall permeability. The first assumption assumes that they are permeable whereas the second assumes that they are not. A statistically significant difference ($p < 10^{-6}$) between the distributions for each permeability assumptions is predicted, and the mean infiltration rate and total heat loss are significantly less for the first assumption than for the second. This shows that an understanding of party wall permeability is both important and relevant, but also introduces uncertainty into the effectiveness of current policies that aim to reduce energy demand through fabric tightening. The predicted distributions of heating season mean infiltration rate and total heat loss for each permeability assumption are useful tools that policy makers of countries whose housing stocks contain multi-family

dwellings can use to make informed decisions about party wall permeability, fabric tightness, and exfiltration heat loss.

The distributions of infiltration rate are used to show that at up to 79% of dwellings could require additional PPV to limit negative health consequences. The distributions of the total heat lost by exfiltration are used to estimate the associated total heating demand for the entire English and UK stocks. Exfiltration is estimated to be responsible for 3-5% of the total UK energy demand, 11-15% of the total energy demand of the UK housing stock and 10-14% of its CO₂e emissions, whatever the party wall permeability assumption. Remediation measures are challenging but could be undertaken alongside other retrofitted energy efficiency measures. It is imperative that sufficient PPV is provided to mitigate negative impacts on occupant health.

The predicted infiltration rates are compared against those made using a *leakage-infiltration ratio*. Concern is raised about its use in building codes because a linear relationship between a measurement of the air leakage rate and the operational infiltration rate during the heating season is not found to be a robust model. This is independent of the dwelling type and the party wall permeability assumption because the LIR cannot account for the variation in geometric, environmental, and physical parameters. The BREDEM and SAP simplified energy models, which apply a LIR and account for some environmental parameters, are also shown to have limitations and so their predictions of heating season infiltration rates and associated heat losses should be treated with caution.

The limiting metrics of scaled Air Leakage Rate specified by building codes do not, in exclusivity, give an indication of expected operational infiltration rates because they are obtained under artificial high-pressure steady-state conditions and do not describe the influence of, or variation in, geometric, environmental, and physical parameters and so are only useful as arbitrary indicators of build quality. A new approach may be required to give a set of useful metrics that can be used to determine mean infiltration rates during the heating season and its associated heating demand.

REFERENCES

- [1] H.M. Government. Climate Change Act. London, U.K. 2008.
- [2] Palmer J, Cooper I. United Kingdom Housing Energy Fact File. Department of Energy & Climate Change; 2013.
- [3] DECC. A summary of the Government's proposals, Technical Report 10D/996. Department of Energy and Climate Change; 2010.
- [4] Dowson M, Poole A, Harrison D, Susman G. Domestic UK retrofit challenge: Barriers, incentives and current performance leading into the Green Deal. *Energy Policy*. 2012;50:294-305.
- [5] Dimitroulopoulou, C. 2012. Ventilation in European dwellings: A review. *Building and Environment* 47(0): 109-125.
- [6] Jokisalo, J., Kalamees, T., Kurnitski, J., Eskola, L., Jokiranta, K. and Vinha, J. 2008. A Comparison of Measured and Simulated Air Pressure Conditions of a Detached House in a Cold Climate. *Journal of Building Physics* 32(1): 67-89.
- [7] Keig P, Hyde T, McGill G. A comparison of the estimated natural ventilation rates of four solid wall houses with the measured ventilation rates and the implications for low-energy retrofits. *Indoor and Built Environment*. 2014.
- [8] Persily, A., Musser, A. and Emmerich, S.J. 2010. Modeled infiltration rate distributions for U.S. housing. *Indoor Air* 20(6): 473-485.
- [9] BSI. 2001. EN13829:2001. Thermal performance of buildings - Determination of air permeability of buildings - Fan pressurization method. British Standards Institution.
- [10] ASTM. 1999. Standard E779: Standard test method for determining air leakage by fan pressurization. 739 American Society of Testing and Materials., Philadelphia, PA, USA.
- [11] CIBSE. 2000. TM23: 2000. Testing buildings for air leakage. London, CIBSE Publications.
- [12] H.M. Government. 2010. The Building Regulations 2000 (2010 edition): Approved Document L1A: Conservation of fuel and power in new dwellings, Crown Copyright 2010.
- [13] Etheridge, D.W. 2012. *Natural Ventilation of Buildings: Theory, Measurement and Design*, John Wiley and Sons.

- [14] Cooper, E.W. and Etheridge, D.W. 2007. Determining the adventitious leakage of buildings at low pressure. Part 1: uncertainties. *Building Services Engineering Research and Technology* 28(1): 71-80.
- [15] Cooper, E.W., Etheridge, D.W. and Smith, S.J. 2007. Determining the adventitious leakage of buildings at low pressure. Part 2: pulse technique. *Building Services Engineering Research and Technology* 28(1): 81-96.
- [16] Sherman MH, Dickerhoff DJ. Airtightness of U.S. dwellings. *ASHRAE Transactions*. 1998;104:1359-67.
- [17] Ministry of the Environment of Finland. 2012. National Building Code of Finland, Part D5: Calculation of power and energy needs for heating of buildings, Department of the Built Environment, Ministry of the Environment, Finland.
- [18] BSI. 1991. BS 5925: Code of Practice for Ventilation Principles and Designing for Natural Ventilation. London, BSI.
- [19] Henderson, J. and Hart , J. 2012. BREDEM 2012 - A technical description of the BRE Domestic Energy Model, hBRE, Garston, Watford.
- [20] Jones, B.M., Das, P., Chalabi, Z., Davies, M., Hamilton, I., Lowe, R.J., Milner, J., Ridley, I., Shrubsole, C. and Wilkinson, P. The Effect of Party Wall Permeability on Estimations of Infiltration from Air Leakage. *International Journal of Ventilation* 12(1): 17-29; 2013.
- [21] Shin, H.K. and Jo, J.H. Air Leakage Characteristics and Leakage Distribution of Dwellings in High-rise Residential Buildings in Korea. *Journal of Asian Architecture and Building Engineering* 12(1): 87-92; 2013.
- [22] Chan W.R, Nazaroff W.W., Price P.N., Sohn M.D., Gadgil A.J. Analyzing a database of residential air leakage in the United States. *Atmospheric Environment*. 2005;39:3445-55.
- [23] Lowe R.J. Ventilation strategy, energy use and CO2 emissions in dwellings - a theoretical approach. *Building Services Engineering Research and Technology*. 2000;21:179-85.
- [24] Lyberg M. Basic air infiltration. *Building and Environment*. 1997;32:95-100.

- [25] Jones BM, Lowe RJ, Davies M, Chalabi Z, Das P, Ridley I. Modelling uniformly porous façades to predict dwelling infiltration rates. *Building Services Engineering Research and Technology*. 2014;35.
- [26] MathWorks. MATLAB Version 8.3.0.532 (R2014a). The MathWorks Inc. 2013
- [27] DOMVENT code available at: <http://tinyurl.com/domvent>.
- [28] ASHRAE. Fundamentals. Atlanta, U.S.A. 2009.
- [29] Day A.R., Knight I., Dunn G., Gaddas R. Improved methods for evaluating base temperature for use in building energy performance lines. *Building Services Engineering Research and Technology*. 2003;24:221-8.
- [30] Hamilton I., Davies M., Ridley I., Oreszczyn T., Barrett M., Lowe R., *et al.* The impact of housing energy efficiency improvements on reduced exposure to cold — the ‘temperature take back factor’. *Building Services Engineering Research and Technology*. 2011;32:85-98.
- [31] Das P., Chalabi Z., Jones B.M., Milner J., Shrubsole C., Davies M., *et al.* Multi-objective methods for determining optimal ventilation rates in dwellings. *Building and Environment*. 2013;66:72-81.
- [32] DCLG. English Housing Survey: Headline report 2009-10. London: Department for Communities and Local Government; 2011.
- [33] DCLG. English Housing Survey Surveyor Briefing Manual. Part 1: Completing the Survey Form. London: Department for Communities and Local Government; 2011.
- [34] Hughes M, Armitage P, Palmer J, Stone A. Converting English Housing Survey Data for Use in Energy Models. Cambridge Architectural Research Ltd. and University College London; 2012.
- [35] Pan W. Relationships between air-tightness and its influencing factors of post-2006 new-build dwellings in the UK. *Building and Environment*. 2010;45:2387-99.
- [36] Stephen R. Airtightness in UK dwellings: BRE's test results and their significance. Building Research Establishment; 1998.
- [37] Orme M, Liddament MW, Wilson A. TN 44: Numerical Data for Air Infiltration and Natural Ventilation Calculations. Air Infiltration and Ventilation Centre; 1998.

- [38] H.M. Government. The Building Regulations 2000 (2010 edition): Approved Document L1A: Conservation of fuel and power in new dwellings. Crown Copyright 2010.
- [39] Swami M, Chandra S. Procedures for Calculating Natural Ventilation Airflow Rates in Buildings. ASHRAE; 1987.
- [40] Sherman M.H., Grimsrud D.T. Infiltration–pressurization correlation: simplified physical modeling. Lawrence Berkeley Laboratory; 1980.
- [41] CIBSE. Guide J - Weather, Solar and Illuminance data. 7 ed. London: CIBSE Publications; 2002.
- [42] Deru M.P., Burns P.J. Infiltration and natural ventilation model for whole building energy simulation of residential buildings. ASHRAE Transactions. 2003;109:801-11.
- [43] Shipworth M., Firth S.K., Gentry M.I., Wright A.J., Shipworth D.T., Lomas K.J. Central heating thermostat settings and timing: building demographics. Building Research & Information. 2009;38:50-69.
- [44] Das P, Shrubsole C, Jones B, Hamilton I, Chalabi Z, Davies M, *et al.* Using probabilistic sampling-based sensitivity analyses for indoor air quality modelling. Building and Environment. 2014;78:171-82.
- [45] ISO. 13790:2008. Energy performance of buildings – Calculation of energy use for space heating and cooling. International Standards Organization. 2008.
- [46] Cheng V, Steemers K. Modelling domestic energy consumption at district scale: A tool to support national and local energy policies. Environmental Modelling & Software. 2011;26:1186-98.
- [47] Firth S.K., Lomas K.J., Wright A.J. Targeting household energy-efficiency measures using sensitivity analysis. Building Research & Information. 2009;38:25-41.
- [48] DECC. A summary of the Government’s proposals, Technical Report 10D/996. Department of Energy and Climate Change; 2010.
- [49] Kirkwood BR, Sterne JAC. 2003. Essential medical statistics. Second Edition. Blackwell Science, Massachusetts, USA.

- [50] Faakye O, Arena L, Griffiths D. Predicting Envelope Leakage in Attached Dwellings. U.S. Department of Energy; 2013.
- [51] H.M. Government. The Building Regulations 2000 (2010 edition): Approved Document F: Ventilation. Crown Copyright 2010.
- [52] Shrubsole C, Ridley I, Biddulph P, Milner J, Vardoulakis S, Ucci M, *et al.* Indoor PM2.5 exposure in London's domestic stock: Modelling current and future exposures following energy efficient refurbishment. *Atmospheric Environment*. 2012;62:336-43.
- [53] Milner J, Shrubsole C, Das P, Jones B, Ridley I, Chalabi Z, *et al.* Home energy efficiency and radon related risk of lung cancer: modelling study. *BMJ*. 2014;348.
- [54] DEFRA. 2013 Government GHG Conversion Factors for Company Reporting: Methodology Paper for Emission Factors. 2013.
- [55] Lomas KJ, Eppel H. Sensitivity analysis techniques for building thermal simulation programs. *Energy and Buildings*. 1992;19:21-44.
- [56] Sherman MH, Modera MP. Comparison of measured and predicted infiltration using the LBL infiltration model. *Measured air leakage of buildings*. Philadelphia: ASTM Special Technical Publication 908; 1986. p. 325-47.

APPENDIX A: DOMVENT3D

This appendix provides an overview of DOMVENT3D, a model of infiltration and exfiltration. The following equations are derived in [25] and are reproduced assuming no mechanical ventilation. The net airflow rate through a system of vertical and horizontal surfaces that comprise the thermal envelop of a building is zero and described by the continuity equation

$$\sum_{i=1}^j \dot{V}_i = 0 \quad (\text{A1})$$

where \dot{V}_i (m^3/s), is the airflow rate through the i^{th} of j vertical and horizontal surfaces. Airflow through a vertical surface \dot{V}_v (m^3/s) of height z_s (m), is given by

$$\dot{V}_v = \dot{V}_1 + \dot{V}_2 \text{ where} \quad (\text{A2})$$

$$\dot{V}_1 = \frac{E(2/\bar{\rho})^b w \varepsilon (\rho_E - \rho_I)}{b + 1} \{ |(\rho_E - \rho_I) | g \}^b \left[\begin{array}{l} +z_0^{b+1} \Big|_{z_0 > z_{min}} \\ -(z_0 - z_{max})^{b+1} \Big|_{z_0 > z_{max}} \end{array} \right] \quad (\text{A3})$$

$$\dot{V}_2 = \frac{E(2/\bar{\rho})^b w \varepsilon (\rho_I - \rho_E)}{b + 1} \{ |(\rho_E - \rho_I) | g \}^b \left[\begin{array}{l} +(z_{max} - z_0)^{b+1} \Big|_{z_0 < z_{max}} \\ -(-z_0)^{b+1} \Big|_{z_0 < z_{min}} \end{array} \right] \quad (\text{A4})$$

Here ρ_E , ρ_I , and $\bar{\rho}$ are the external, internal, and mean air densities (kg/s), respectively, z_{max} and z_{min} are the are the top and bottom surface heights (m) above ground level (so that $z_s = z_{max} - z_{min}$), respectively, w is the surface width (m), b is a flow exponent, and g is the gravitational acceleration (m/s^2). The flow direction function $\varepsilon(x) = 1$ if $x > 0$, $\varepsilon(x) = -1$ if $x < 0$, and $\varepsilon(x) = 0$ if $x = 0$. The surface neutral height z_0 (m) is given by

$$z_0 = \frac{\frac{1}{2} \rho_E u^2 c_p - p_I}{(\rho_E - \rho_I) g} \quad (\text{A5})$$

where u is the wind speed (m/s) at building height z_u (m), c_p is the surface wind pressure coefficient, and p_I is the gauge internal air pressure (Pa). The airflow rate through a horizontal surface \dot{V}_h (m^3/s), is given by

$$\dot{V}_h = (Ewd(2/\bar{\rho})^b) |\{\rho_I - \rho_E\}gz - p_I|^b \varepsilon(\{\rho_I - \rho_E\}gz - p_I) \quad (\text{A6})$$

Where d is the surface depth (m) and z is the surface height (m). In all relevant equations E is a dimensionless relative leakage area given by

$$E = \frac{Q_{50}A}{3600A_{50}(100/\rho_{STP})^b} \quad (\text{A7})$$

Where ρ_{STP} (kg/m^3) is the air density at standard temperature and pressure, A (m^2) is the dwelling envelope area, Q_{50} ($\text{m}^3/\text{h}/\text{m}^2$) is the air permeability measured at $\Delta P = 50\text{Pa}$, and A_{50} (m^2) is the dwelling's permeable $\Delta P = 50\text{Pa}$.

APPENDIX B: SOURCES OF DATA

Tables B1, B2, and B3 to be placed here.

FIGURES

Figure 1: English housing stock by type.

Figure 2: Predicted cumulative distributions and probability density functions of mean heating season infiltration rate \bar{N} (h^{-1}) for the English housing stock. —, Assumption $A(\tilde{Q} = 1)$; ·····, assumption $A(\tilde{Q} = 0)$.

Figure 3: Predicted cumulative distributions and probability density functions of total heat loss H_I (kWh) during the heating season for the English housing stock. —, Assumption $A(\tilde{Q} = 1)$; ·····, assumption $A(\tilde{Q} = 0)$.

Figure 4: Predicted distributions of the mean heating season infiltration rate \bar{N} (h^{-1}) and total heat loss H_I (MWh) during the heating season for permeable and impermeable party walls by dwelling type and stock. A, apartments; MT, mid-terrace; ET, end-terrace; SD, semi-detached; D, detached; ALL, stock.

Figure 5: Predicted cumulative distributions of mean heating season infiltration rate \bar{N} (h^{-1}) for the English housing stock. Black, $A(\tilde{Q} = 1)$; Cyan, $A(\tilde{Q} = 0)$; Blue, BREDEM; Green, SAP; Red, $L=20$.

Figure 6: Sensitivity of model outputs to inputs. Q_{50} , air permeability; b , flow exponent; $A_I: A_{50}$, area of façade permeable under operational conditions : area of façade permeable at 50Pa; u , mean wind speed; α , dwelling orientation; $A: V$, dwelling envelope area : volume; AR , block aspect ratio; ΔT , mean difference between internal and external temperatures.

FIGURE 1

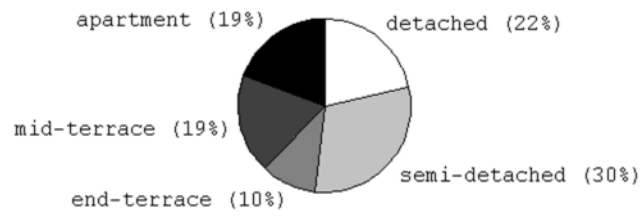


FIGURE 2

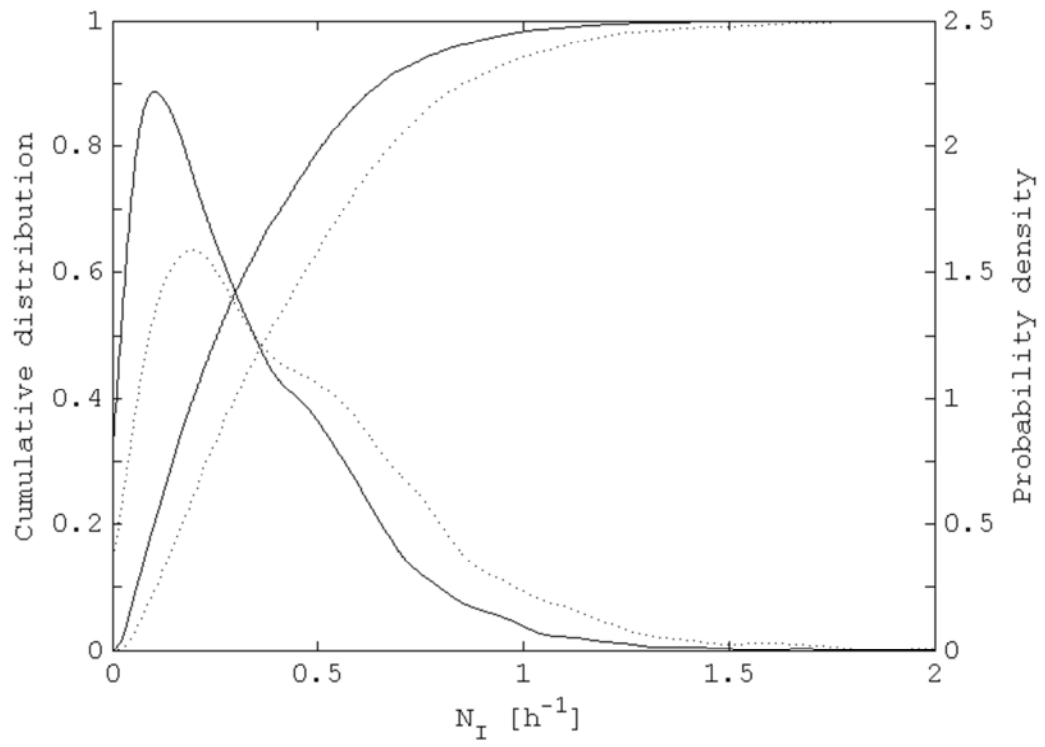


FIGURE 3

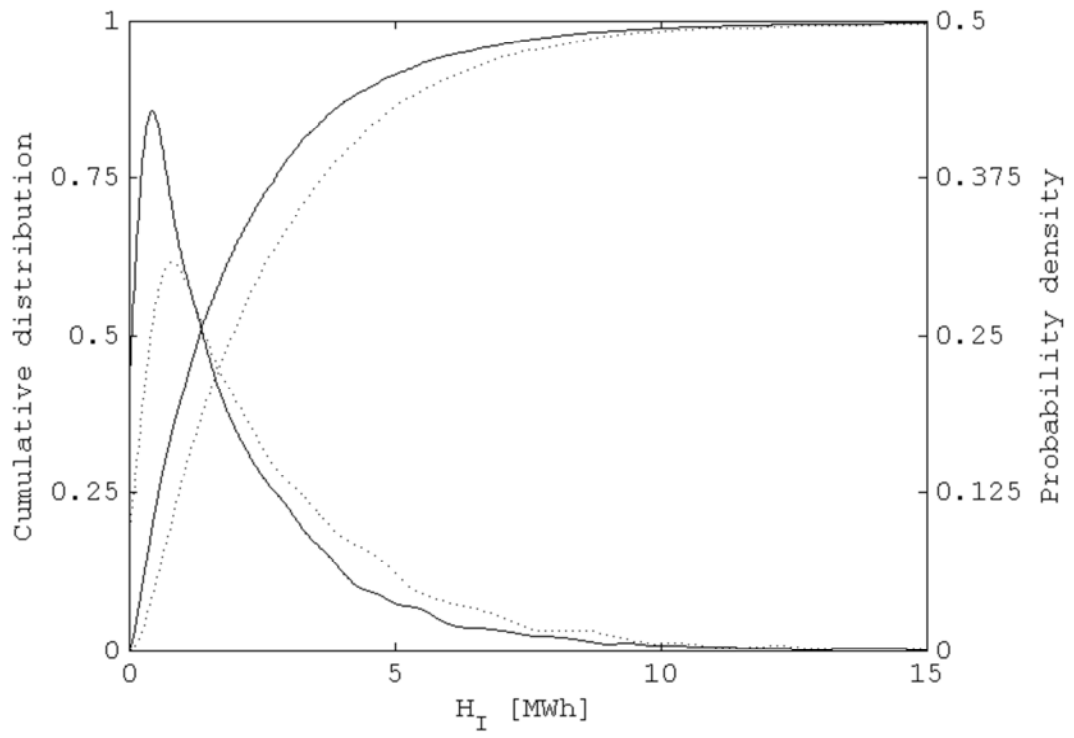


FIGURE 4

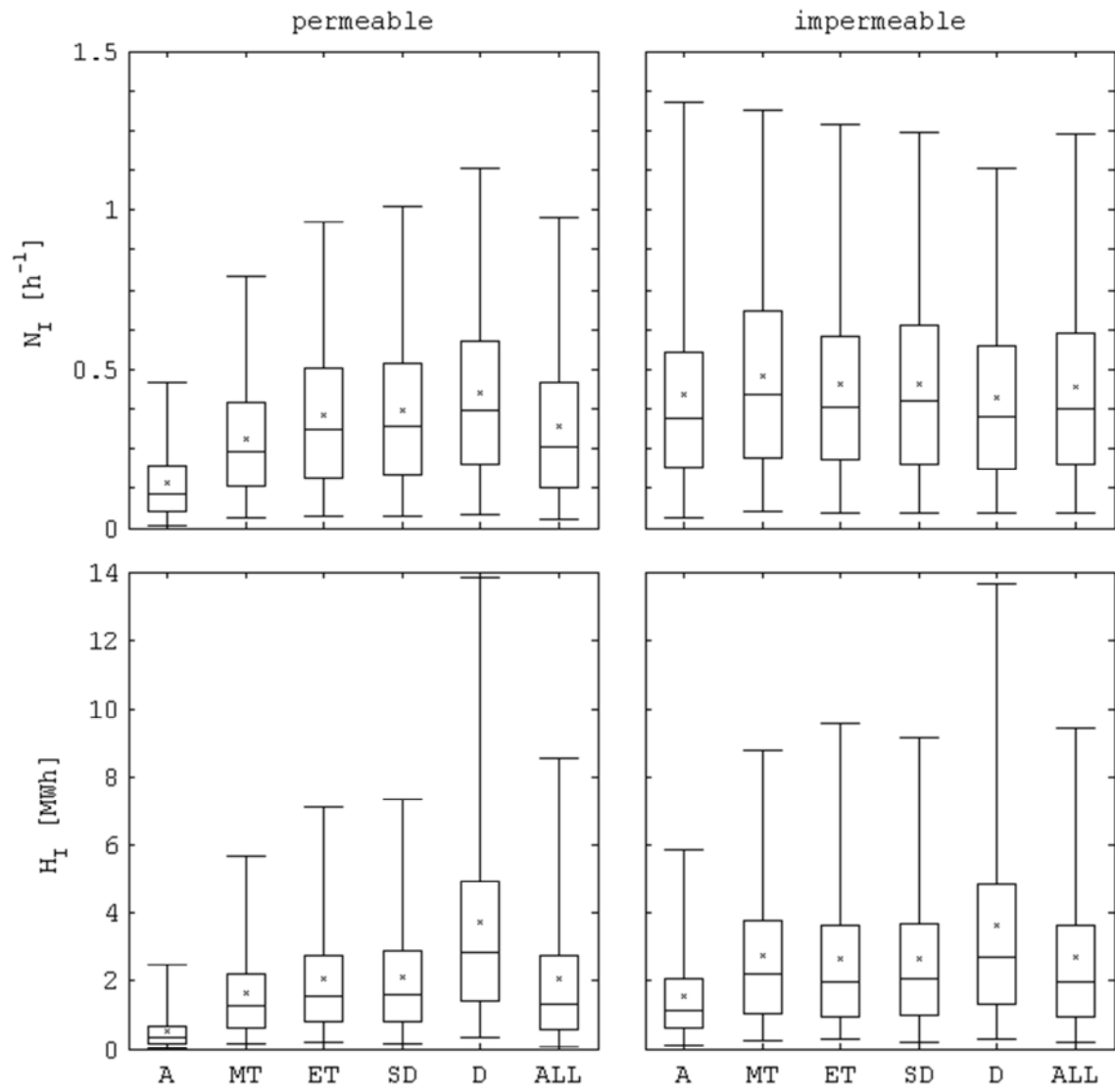


FIGURE 5 [Intended for colour reproduction]

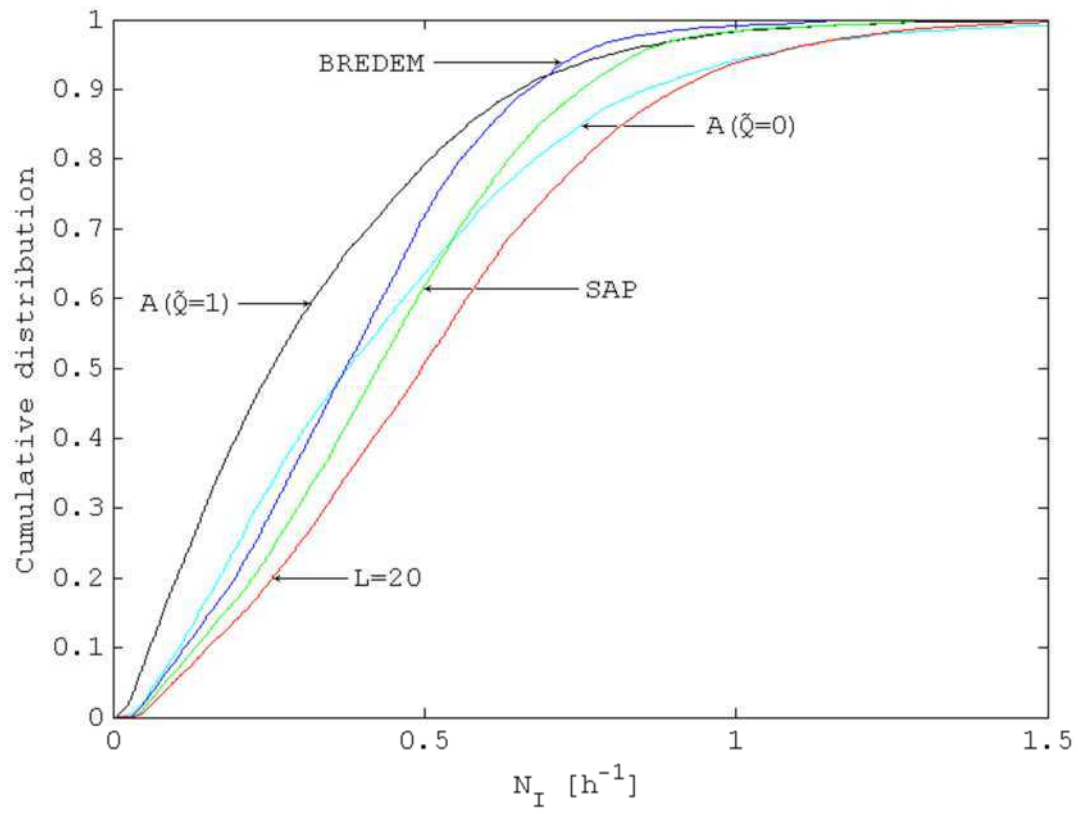
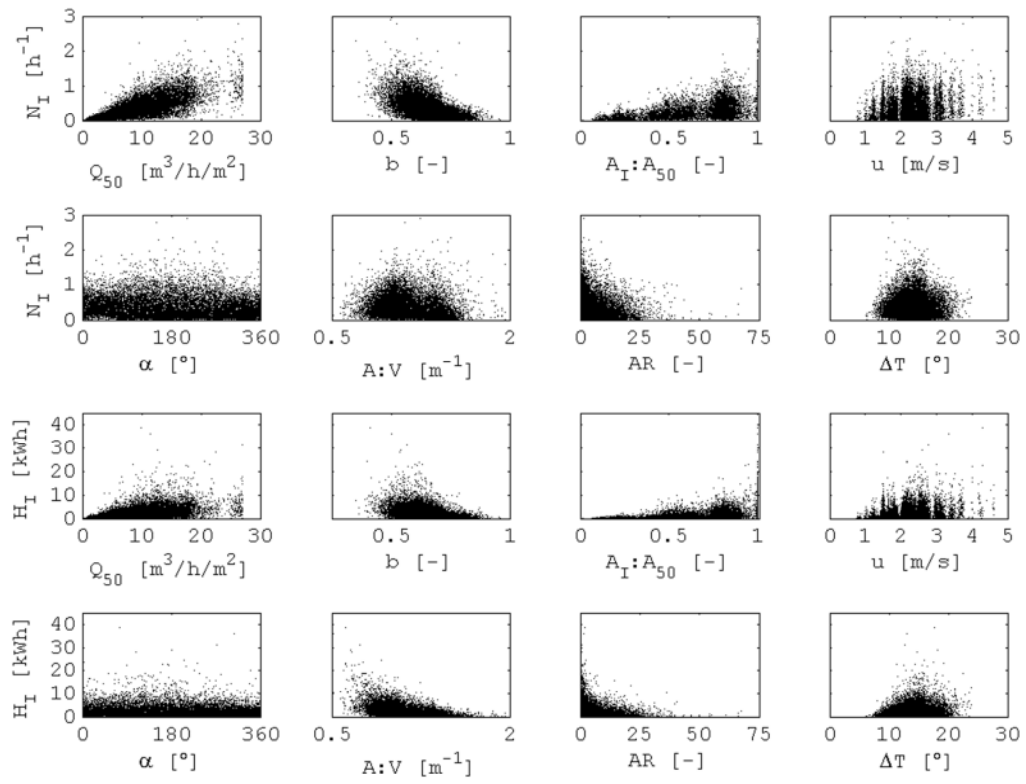


FIGURE 6



TABLES

Table 1: Statistical summary of mean heating season infiltration rate (h^{-1}) by dwelling type and stock.

Assumption $A(\tilde{Q} = 1)$: permeable party walls. Assumption $A(\tilde{Q} = 0)$: impermeable party walls.

Table 2: Statistical summary of total heating season heat loss (MWh) by dwelling type and stock.

Assumption $A(\tilde{Q} = 1)$: permeable party walls. Assumption $A(\tilde{Q} = 0)$: impermeable party walls.

Table 3: Median values of key descriptive parameters of sampled dwellings. Assumption $A(\tilde{Q} = 0)$:

permeable party walls. Assumption $A(\tilde{Q} = 0)$: impermeable party walls.

Table 4: Ranking of input variables according to the sensitivity of the predicted mean heating season infiltration rate (h^{-1}) to them using the format *rank(ranking statistic)* where a rank of 1 is the highest.

Table 5: Ranking of input variables according to the sensitivity of the predicted total heating heat loss (MWh) to them using the format *rank(ranking statistic)* where a rank of 1 is the highest.

Table 6: Predicted leakage infiltration ratio L and performance statistics. Assumption $A(\tilde{Q} = 1)$:

permeable party walls. Assumption $A(\tilde{Q} = 0)$: impermeable party walls.

Table B1: Geometric Inputs

Table B2: Physical Inputs

Table B3: Environmental Inputs

TABLE 1

Type	Apartment		Mid-terrace		End-terrace		Semi-detached		Detached		All		$L = 20$	SAP	BREDEM
Assumption	$A(\tilde{Q} = 1)$	$A(\tilde{Q} = 0)$													
Minimum	0.00	0.00	0.01	0.02	0.01	0.02	0.01	0.01	0.01	0.01	0.00	0.00	0.01	0.01	0.01
2%	0.01	0.03	0.03	0.05	0.04	0.05	0.04	0.05	0.04	0.05	0.02	0.05	0.06	0.06	0.05
25%	0.05	0.19	0.13	0.22	0.16	0.22	0.17	0.20	0.20	0.19	0.13	0.20	0.30	0.26	0.23
50%	0.11	0.35	0.24	0.42	0.31	0.38	0.32	0.40	0.37	0.35	0.26	0.38	0.50	0.43	0.37
75%	0.19	0.55	0.40	0.68	0.51	0.60	0.52	0.64	0.59	0.57	0.46	0.61	0.70	0.59	0.52
98%	0.46	1.34	0.79	1.31	0.96	1.27	1.01	1.25	1.13	1.13	0.98	1.24	1.23	0.97	0.87
Maximum	0.95	2.90	1.23	1.99	1.45	1.88	1.89	2.05	2.77	2.24	2.77	2.90	2.45	1.54	1.56
μ	0.14	0.42	0.28	0.48	0.35	0.45	0.37	0.45	0.43	0.41	0.32	0.44	0.52	0.44	0.39
σ	0.12	0.33	0.20	0.32	0.24	0.32	0.26	0.32	0.29	0.29	0.25	0.31	0.29	0.24	0.21
Sample (n)	1739	1877	1711	1904	912	1064	2757	3148	1881	2207	9000	10200	19200	19200	19200

TABLE 2

Type	Apartment		Mid-terrace		End-terrace		Semi-detached		Detached		All	
Assumption	$A(\tilde{Q} = 1)$	$A(\tilde{Q} = 0)$	$A(1\tilde{Q} = 1)$	$A(\tilde{Q} = 0)$	$A(\tilde{Q} = 1)$	$A(\tilde{Q} = 0)$						
Minimum	0.04	0.04	0.07	0.09	0.00	0.00	0.04	0.04	0.07	0.09	0.00	0.00
2%	0.18	0.23	0.33	0.30	0.08	0.21	0.18	0.23	0.33	0.30	0.08	0.21
25%	0.83	0.99	1.43	1.32	0.56	0.95	0.83	0.99	1.43	1.32	0.56	0.95
50%	1.61	2.05	2.84	2.71	1.33	1.95	1.61	2.05	2.84	2.71	1.33	1.95
75%	2.90	3.68	4.92	4.84	2.75	3.64	2.90	3.68	4.92	4.84	2.75	3.64
98%	7.35	9.13	13.84	13.66	8.55	9.46	7.35	9.13	13.84	13.66	8.55	9.46
Maximum	22.80	20.09	31.04	38.63	31.04	38.63	22.80	20.09	31.04	38.63	31.04	38.63
μ	2.13	2.67	3.73	3.62	2.05	2.70	2.13	2.67	3.73	3.62	2.05	2.70
σ	1.88	2.33	3.33	3.51	2.28	2.59	1.88	2.33	3.33	3.51	2.28	2.59

TABLE 3

Type Assumption	Apartment		Mid-terrace		End-terrace		Semi-detached		Detached		All	
	$A(\tilde{Q} = 1)$	$A(\tilde{Q} = 0)$										
Permeability, Q_{50} (m ³ /h/m ²)	9.0	8.6	8.9	8.8	8.7	8.9	9.2	9.1	9.1	9.1	9.0	8.9
Volume, V (m ³)	141.8	140.4	211.9	211.9	217.6	213.6	216.9	217.5	313.3	308.6	214.5	214.8
Envelope area, A (m ²)	191.3	190.9	228.9	228.4	226.9	224.1	230.6	230.6	307.1	309.9	233.6	233.0
Permeable area under operational conditions, A_I (m ²)	55.4	54.5	124.2	123.1	161.5	158.7	169.8	170.0	256.0	254.6	153.3	153.8
Permeable area at 50Pa, A_{50} (m ²)	175.3	54.5	206.8	123.1	199.9	158.7	205.2	170.0	256.2	254.6	208.8	153.8
$A:V$ (m ⁻¹)	1.3	1.4	1.1	1.1	1.0	1.0	1.1	1.1	1.0	1.0	1.1	1.1
$A_{50,A(\tilde{Q}=1)}:A_{50,A(\tilde{Q}=0)}$	0.31		0.59		0.78		0.83		1.00		0.74	
$\bar{N}_{I,A(1)}:\bar{N}_{I,A(2)}$	0.31		0.57		0.81		0.80		1.06		0.68	

TABLE 4

Input\Test	S_{Kend}	S_{Pear}	S_{Spear}	$S_{regress}$	$S_{rankreg}$	S_{Kolm}	S_{Krusk2}	S_{Krusk5}	$S_{Krusk10}$	$S_{Krusk20}$
Q_{50}	1 (0.59)	1 (0.74)	1 (0.78)	1 (0.74)	1 (0.78)	1 (0.60)	1 (8007)	1 (10956)	1 (11533)	1 (11655)
b	2 (-0.37)	2 (-0.53)	2 (-0.54)	2 (-0.53)	2 (-0.54)	2 (0.43)	2 (2957)	2 (5611)	2 (5844)	2 (5972)
$A_I:A_{50}$	3 (0.23)	3 (0.32)	3 (0.31)	3 (0.32)	3 (0.31)	3 (0.16)	3 (1235)	3 (1717)	3 (1858)	3 (1994)
u	4 (0.11)	4 (0.19)	4 (0.17)	4 (0.19)	4 (0.17)	4 (0.11)	4 (273)	4 (462)	4 (659)	4 (732)
$A:V$	5 (-0.08)	7 (-0.09)	5 (-0.12)	7 (-0.09)	5 (-0.12)	6 (0.09)	6 (258)	5 (375)	5 (446)	6 (474)
α	6 (-0.08)	6 (-0.10)	6 (-0.12)	6 (-0.10)	6 (-0.12)	5 (0.10)	5 (269)	6 (310)	6 (342)	5 (348)
AR	7 (-0.07)	5 (-0.10)	7 (-0.11)	5 (-0.10)	7 (-0.11)	7 (0.07)	7 (158)	7 (230)	7 (250)	8 (256)
ΔT	8 (0.01)	8 (0.03)	8 (0.01)	8 (0.03)	8 (0.01)	8 (0.04)	8 (6)	8 (163)	8 (186)	7 (197)

TABLE 5

Input\Test	S_{Kend}	S_{Pear}	S_{Spear}	$S_{regress}$	$S_{rankreg}$	S_{Kolm}	S_{Krusk2}	S_{Krusk5}	$S_{Krusk10}$	$S_{Krusk20}$
Q_{50}	1 (0.44)	1 (0.50)	1 (0.62)	1 (0.50)	1 (0.62)	1 (0.46)	1 (5263)	1 (7000)	1 (7253)	1 (7366)
b	2 (-0.33)	3 (-0.43)	2 (-0.49)	3 (-0.43)	2 (-0.49)	2 (0.37)	2 (2615)	2 (4450)	2 (4707)	2 (4778)
$A_I:A_{50}$	4 (0.25)	4 (0.29)	4 (0.33)	4 (0.29)	4 (0.33)	6 (0.14)	4 (1407)	4 (2079)	4 (2397)	4 (2547)
u	5 (0.15)	5 (0.24)	5 (0.23)	5 (0.24)	5 (0.23)	4 (0.16)	6 (511)	5 (862)	5 (1008)	5 (1084)
$A:V$	3 (-0.33)	2 (-0.44)	3 (-0.47)	2 (-0.44)	3 (-0.47)	3 (0.30)	3 (2569)	3 (3713)	3 (4263)	3 (4462)
α	8 (-0.09)	8 (-0.12)	8 (-0.14)	8 (-0.12)	8 (-0.14)	8 (0.11)	7 (327)	8 (389)	8 (423)	8 (441)
AR	6 (-0.15)	7 (-0.17)	6 (-0.22)	7 (-0.17)	6 (-0.22)	7 (0.13)	5 (609)	6 (823)	6 (913)	6 (948)
ΔT	7 (0.11)	6 (0.19)	7 (0.17)	6 (0.19)	7 (0.17)	5 (0.14)	8 (192)	7 (605)	7 (687)	7 (739)

TABLE 6

	A($\tilde{Q} = 1$)				A($\tilde{Q} = 0$)			
	L	R^2	RMSE	MAE	L	R^2	RMSE	MAE
apartment	68.87	0.01	6.79	46.69	24.15	0.13	6.33	45.94
mid-terrace	32.11	0.51	3.96	21.35	18.70	0.55	3.65	15.11
end-terrace	25.01	0.60	3.48	14.11	19.07	0.57	3.61	16.33
semi-detached	24.25	0.45	4.21	25.38	19.66	0.49	4.06	24.68
detached	19.86	0.44	3.96	25.80	19.82	0.42	3.99	20.39
all	25.67	-0.05	6.06	41.88	20.22	0.39	4.56	34.53

TABLE B1

Input (symbol)	Units	Value(s), comment, or PDF assumed	Source
Dwelling surface width, depth, height, and top and bottom heights above ground level ($w, d, z_s, z_{max}, z_{min}$)	m	Defined by EHS for each storey and surface. Constructed following the Cambridge Housing Model.	[32] [34]
Block aspect ratio	-	Product of (w/d) and the number of houses in a block or terrace.	
Apartment block floors	-	Number of floors in a block of apartments.	[32]
Number of houses in a terrace		$U(3,20)$	
Location in an apartment block, (X, Y)	-	For apartments only. X: if the dwelling has 3 sides or 2 perpendicular sides, then the dwelling is assumed to be located at the edge of a block. If the dwelling has one façade or two opposite façades then the dwelling is a uniformly random location along the block's width. Y: a uniformly random variable between the lowest (basement or ground floor) and the highest storey.	
Dwelling orientation (α)	°	$U(0,360)$	
Dwelling height (z_u)	m	The ceiling height of the top floor of the dwelling.	[32]
Dwelling type	-	Apartment, end-terrace, mid-terrace, semi-detached, detached.	[32]

TABLE B2

Input (symbol)	Units	Value(s), comment, or PDF assumed	Source
Permeability (Q_{50})	$\text{m}^3/\text{h}/\text{m}^2$	$f(\text{dwelling age})$ pre-2000, post-2000.	[36], [35]
Party wall relative permeability \tilde{Q}	-	Party walls have a permeability equivalent to a dwelling when $\tilde{Q} = 1$ and are impermeable when $\tilde{Q} = 0$.	
Dwelling age	years	EHS parameter indicating construction pre-2000 and post-2000	[32]
Airflow exponent (b)	-	$N(0.651, 0.077)$	[16]
Façade wind pressure coefficient (C_p)	-	$f(\theta, w, z_u, d, C_{p0})$ Low-rise dwelling, High-rise dwelling.	[39]; [38]
Wind pressure coefficient for front surfaces of dwelling with wind normal to them (C_{p0})		$f(\text{sheltering})$. Product of 0.6 and the LBL shielding factor. For basement apartments no wind driven infiltration is assumed; then $C_{p0} = 0$.	[39] [56]

TABLE B3

Input (symbol)	Units	Value(s), comment, or PDF assumed	Source
Dwelling location	-	EHS region (CIBSE region){BREDEM region}: North East (Newcastle){Thames}, North West (Manchester){North West}, Yorkshire and the Humber (Leeds){East Pennines}, East Midlands (Nottingham){Midlands}, West Midlands (Birmingham){Midlands}, East (Norwich){East Anglia}, London (London){Thames}, South East (Southampton){South}, South West (Plymouth{South West} or Swindon{Severn} [chosen as a uniform random variable])	[32] [41] [19]
Altitude (h)	m	$f(location)$. Given by weather file.	[41]
Wind direction (θ)	°	$f(location)$. Given by weather file.	[32]; [41]
Weather station wind speed (u_0)	m/s	$f(location)$	[41]
Terrain coefficients (k, m)	-	$f(location, sheltering)$	[18]; [32]
Wind speed at dwelling height (u)	m/s	$f(u_0, z_u, k, m, location)$	[18]
Sheltering	-	EHS sheltering {LBL shielding coefficient}[BSI terrain coefficients] BREDEM : City {very heavy shielding}[city] city , Urban {heavy shielding}[urban] average , Suburban {heavy shielding}[urban] average , Rural residential {moderate local shielding}[urban] average , Village centre {moderate local shielding}[urban] average , Rural {light local shielding}[scattered wind breaks] average special case: apartment on 10 th floor or above, exposed special case: apartment on 6-9 th floors, above average special case: sheltered 3 storey houses, below average	[32] {[56]; [42]} [[18]] [19]
Internal dry bulb temperature (T_{int})	°C	$N(21.1, 2.5)$	[43]
External dry bulb temperature (T_{ext})	°C	$f(location)$. Given by weather file.	[41]